Published in final edited form as:
Pain. 2011 November ; 152(11): 2564–2574. doi:10.1016/j.pain.2011.07.020.

Preventive or late administration of anti-NGF therapy attenuates tumor-induced nerve sprouting, neuroma formation and cancer pain

Juan Miguel Jimenez-Andrade[a], **Joseph R. Ghilardi**[b], **Gabriela Castaneda-Corral**[a], **Michael A. Kuskowski**[c], and **Patrick W. Mantyh**[a,b,d]

[a]Department of Pharmacology, College of Medicine, University of Arizona, Tucson, AZ 85724, USA

[b]Research Service, VA Medical Center, Minneapolis, MN 55417, USA

[c]GRECC, VA Medical Center, One Veterans Drive, Minneapolis, MN 55417, USA

[d]Arizona Cancer Center, University of Arizona, Tucson, AZ 85724, USA

Abstract

Early, preemptive blockade of nerve growth factor (NGF)/Tropomyosin receptor kinase A (TrkA) attenuates tumor-induced nerve sprouting and bone cancer pain. A critical unanswered question is whether late blockade of NGF/TrkA can attenuate cancer pain once NGF-induced nerve sprouting and neuroma formation has occurred. Using a mouse model of prostate cancer-induced bone pain, anti-NGF was either administered preemptively at day 14 post-tumor injection when nerve sprouting had yet to occur or late at day 35 when extensive nerve sprouting had occurred. Animals were sacrificed at day 70 when, in vehicle-treated animals, significant nerve sprouting and neuroma formation was present in the tumor-bearing bone. While preemptive/sustained administration (days 14 – 70) of anti-NGF more rapidly attenuated bone cancer nociceptive behaviors than late/sustained administration (days 35 – 70), by day 70 post-tumor injection both preemptive and late administration of anti-NGF significantly reduced nociceptive behaviors, sensory and sympathetic nerve sprouting, and neuroma formation. In this model, as in most cancers, the individual cancer cell colonies have a limited half-life as they are constantly proliferating, metastasizing and undergoing necrosis as the parent cancer cell colony outgrows its blood supply. Similarly, the sensory and sympathetic nerve fibers that innervate the tumor undergo sprouting at the viable/leading edge of the parent tumor, degenerate as the parent cancer cell colony becomes necrotic, and re-sprout in the viable, newly formed daughter cell colonies. These results suggest that preemptive or late stage blockade of NGF/TrkA can attenuate nerve sprouting and cancer pain.

Corresponding author: Patrick W. Mantyh, Ph D, Department of Pharmacology, College of Medicine, University of Arizona, 1656 E. Mabel, Rm. #119, PO Box 245215, Tucson, AZ 85724, Phone: (520) 626-0742, Fax: (520) 626-8869, pmantyh@email.arizona.edu.

Conflicts of interest statement

None of the authors of this study claim a conflict of interest.

Keywords

bone; analgesia; prostate cancer; neuroplasticity

1. Introduction

In 2010 over 12 million cancer cases (excluding non-melanoma skin cancer) and 7.6 million cancer deaths occurred worldwide [22]. Improvements in the detection and treatment of most cancers have increased survival rates so that even patients diagnosed with metastatic cancer can survive years to decades beyond their initial diagnosis [23]. For many patients, pain is not only the first sign of cancer but can significantly impact their quality of life and functional status [15,47]. While cancer-associated pain can be present at any time during the course of the disease, the frequency, severity and difficulty in controlling cancer pain tends to increase with advancing stages of cancer so that 75 to 90% of patients with metastatic or advanced stage cancer will experience significant cancer-induced pain [10,54,56].

Although cancer pain is common, our current understanding of the mechanisms that drive cancer pain are incomplete as is our ability to fully control advanced cancer pain without significant unwanted side effects [6,38,41]. A number of factors have frustrated efforts to develop mechanism-based therapies to more effectively control chronic cancer pain. These include lack of animal models that mirror cancer pain that arises from different types of cancer [33,39], the poor correlation between tumor burden and the severity of pain [14,31,40], and the lack of understanding as to how sensory and sympathetic nerve fibers that innervate the tumor-bearing organ change with disease progression.

These challenges notwithstanding, recent research has revealed that cancer pain is not simply due to inflammation at the tumor site but that rather cancer pain is driven by tumor-induced acidosis [17], products released by cancer cells and their associated stromal cells (for review see [33,48]), and tumor-induced injury to peripheral nerve fibers that innervate the tumor-bearing organ [42]. Previous *in-vitro* and *in-vivo* studies have shown that tumors can induce a significant and pathological sprouting of sensory and sympathetic nerve fibers that innervate the tumor-bearing tissue [2,4,8,24,32,34,51,57]. However, what remains unclear is if the cancer cell colonies are constantly growing, undergoing necrosis and metastasizing to new sites, are the sensory and sympathetic nerve fibers that innervate the tumor bearing organ also continually changing and what does this imply for our understanding and treatment of cancer pain?

To begin to explore these questions, a mouse model of prostate cancer-induced bone pain was employed as this model can be assessed up to 70 days post-tumor injection by which time parent cancer cell colonies have proliferated, undergone necrosis and given rise to new daughter cell colonies. Using this model it is shown here that both sensory and sympathetic nerve fibers undergo significant sprouting and neuroma formation when the parent cell colony is viable, but these nerve fibers degenerate as the parent cancer cell colonies undergo necrosis, and then re-sprout at the leading, viable edge of new daughter cancer cell colonies. These results suggest that just as the cancer cell colonies are continually evolving with disease progression so are the sensory and sympathetic nerve fibers that innervate the tumor-bearing organ.

2. Materials and Methods

2.1 Mice

Experiments were performed using 41 adult male athymic nude mice (8–10 weeks old, Harlan Laboratories, Madison, WI), weighing 20 to 32 g. The mice were housed in accordance with the NIH guidelines under specific pathogen-free conditions in autoclaved cages maintained at 22°C with a 12 hr alternating light and dark cycle and were given autoclaved food and water *ad libitum*. All procedures adhered to the guidelines of the Committee for Research and Ethical Issues of the IASP [61] and were approved by the Institutional Animal Care and Use Committee at the University of Arizona (Tucson, AZ) and VA Medical Center (Minneapolis, MN).

2.2 Tumor cell inoculation surgery

Canine prostate carcinoma (ACE-1) cells were stably transfected with green fluorescent protein (GFP), cultured and injected into the intramedullary space as previously described [18]. These canine GFP expressing prostate cancer cells grow relatively slowly, are remarkably bone seeking, and do not appear to avidly metastasize to other organs than bone [24,30]. Briefly, following induction of general anesthesia with ketamine/xylazine (100/5 mg/kg, i.p.), an arthrotomy was performed exposing the condyles of the distal femur. The bone was cored with a 30 gauge needle inserted at the level of the intercondylar notch. The coring needle was then replaced with a 29 gauge hypodermic needle used to inject either sterile Hank's buffered salt solution (HBSS, Sigma, 20 μl; n=9) as the control or HBSS containing 10^5 ACE-1 GFP cells (20 μl; n=32) into the intramedullary space. In order to prevent cell reflux following injection, the injection site was sealed with dental grade amalgam (Dentsply) using an endodontic messing gun (Union Broach). The injection site was then irrigated with sterile filtered water (hypotonic solution) and wound closure was achieved using a single 7 mm auto wound clip (Becton Dickinson).

2.3 Evaluation of spontaneous nociceptive behaviors and tumor-induced bone remodeling

Mice were behaviorally tested at days 0, 14, 21, 28, 35, 42, 49, 56, 63 and 70 post-cancer cell or HBSS (culture medium) injection. Using immunohistochemisty, at 70 days post-tumor cell injection there were necrotic cancer colonies and viable cancer colonies in the tumor-bearing bone. Furthermore, we could not detect any GFP^+ prostate tumor cells that spread to other organs such as liver, lung, brain, GI tract etc. Because these tumor cells preferentially grow in bone, this makes behavioral testing for pain feasible as the tumor appears to be growing only in the original tumor injected femur and the general health of the animal (as judged by weight loss, grooming, feeding, luster of coat, etc) does not appear to be significantly impaired. Mice were placed in a clear plastic observation box with a wire mesh floor and allowed to habituate for a period of 30 min. After acclimation, the number of spontaneous flinches and the time spent guarding the tumor-bearing limb were recorded over a 2 min observation period [18,46]. Flinches were defined as holding the hindpaw aloft while not ambulatory. Guarding was defined as the time the hindpaw was held aloft while ambulatory. These spontaneous behaviors were examined to reflect the clinical condition when patients with metastatic prostate cancer experience spontaneous bone pain and protect the tumor-bearing limb [43].

In order to characterize the cancer-induced changes in mineralized bone, radiographic analysis was performed immediately after behavioral analysis at the same time points previously stated. Mice were lightly anesthetized (2% isoflurane) and digital radiographs (MX20 DC12, Faxitron X-Ray Corporation, Wheeling, IL, USA) of lower extremities were obtained. Radiograph images of the medial-lateral plane of ipsilateral femurs were used to visualize tumor-induced bone remodeling.

2.4 Experimental groups

Prostate cancer-injected mice were divided into 4 groups: prostate cancer + vehicle (sacrificed at day 35; n=8), prostate cancer + vehicle (sacrificed at day 70; n=7), prostate cancer + early/sustained anti-NGF (administered every 5 days from day 14 until day 70 and sacrificed at day 70; n=8), prostate cancer + late/sustained anti-NGF treatment (administered every 5 days from day 35 until day 70 and sacrificed at day 70; n=9). The anti-nerve growth factor (NGF) sequestering antibody (mAb 911), kindly provided by Dr. David Shelton (Rinat/Pfizer), is effective in blocking the binding of NGF to both Tropomyosin receptor kinase A (TrkA) and p75 NGF receptors and inhibiting TrkA autophosphorylation [20]. The anti-NGF antibody possesses a plasma half-life of approximately 5–6 days in the mouse and it does not appreciably cross the blood brain barrier [53]. The dose used in this study (10 mg/kg, i.p.) has been shown to be efficacious at attenuating bone cancer-induced pain in mouse models [18,52]. Therapy was initiated either when cancer-induced nociceptive behaviors were first evident and nerve sprouting has yet to occur (day 14) or after significant disease progression and nerve sprouting had occurred (day 35). The general health of the mice was closely monitored using food consumption and body weight as general health indicators throughout the experiments.

2.5 Immunohistochemistry

At days 35 and 70 post-cancer cell injection mice were deeply anesthetized using CO_2 delivered from a compressed gas cylinder and perfused intracardially with 20 ml of 0.1M phosphate buffered saline (PBS, pH=7.4 at 4°C) followed by 30 ml of 4% formaldehyde/ 12.5% picric acid solution in 0.1M PBS (pH=6.9 at 4°C). Mouse femurs were removed, post-fixed for 24 hr in the perfusion fixative, rinsed with PBS and decalcified in 10% ethylenediaminetetraacetic acid (EDTA) at 4°C. EDTA was changed once a week for two weeks or until total decalcification, which was radiographically monitored using a Faxitron MX20 cabinet X-ray system (Faxitron X-Ray Corporation, Wheeling, IL, USA) and Kodak MinR 2000 film (Eastman Kodak Co., Windsor, CO, USA). Once decalcification had occurred, the bones were cryoprotected in 30% sucrose and serially sectioned along the longitudinal axis, in the coronal plane, at a thickness of 20 μm. Bone sections were mounted on gelatin-coated slides, dried at room temperature for 30 min, rinsed with 0.1M PBS (3X10 min) blocked with 3% normal donkey serum (NDS) and 0.3% triton-X-100 in PBS for 1 hr and incubated with primary antibodies overnight. Primary antibodies were made in a solution of 1% NDS and 0.1% triton X-100 in PBS. Peptide-rich sensory nerve fibers were labeled with an antibody against calcitonin-gene related peptide (CGRP, polyclonal rabbit anti-rat CGRP; 1:10,000, Sigma Chemical Co., St. Louis, MO, catalog #C8198). Myelinated sensory nerve fibers were labeled with an antibody against neurofilament 200 kDa (NF200, chicken anti-NF200, 1:5000, Neuromics, Edina, MN, catalog #CH20014). Sympathetic nerve fibers were labeled with an antibody against tyrosine hydroxylase (TH, polyclonal rabbit anti-rat TH, 1:1,000, Chemicon, Temecula, CA, catalog #AB152). Nerve fibers expressing the tropomyosin receptor kinase A (TrkA) were labeled with an antibody against TrkA (goat anti-TrkA, 1:50, R&D Systems, Minneapolis, MN, catalog #AF1056). Blood vessels were labeled with an antibody against the platelet endothelial cell adhesion molecule (PECAM, rat anti-mouse CD31, 1:500, BD PharMingen, San Diego, CA, catalog #550274). Monocytes/macrophages were identified with an antibody against a single chain glycoprotein of 110kD that is expressed predominantly on the lysosomal membrane of myeloid cells (rat anti-mouse CD68; 1:2000, AbD Serotec, Oxford, UK, catalog #MCA1957). Following primary antibody incubation, the slides were washed with 0.1M PBS (3X10 min). Since endogenous GFP signal from cancer cells was visualized in the green channel (band-pass emission filter from 500 to 530 nm), preparations were then incubated with Cy3- or Cy5-conjugated secondary antibodies (1:600 and 1:400, respectively, Jackson ImmunoResearch) for 3 hr. Preparations were then washed with 0.1M

PBS (3X10 min) and counterstained with DAPI (4′, 6-diamidino-2-phenyl-indole, dihydrochloride, 1:30000, Invitrogen/Molecular Probes) for 5 min and washed with 0.1M PBS (3X10 min). Finally, tissue was dehydrated through an alcohol gradient (70, 80, 90, and 100%) for 2 min per gradient, cleared in xylene (2X2 min) and coverslipped with di-n-butylphthalate-polystyrene-xylene (Sigma). Preparations were allowed to dry at room temperature for 12 hrs before imaging. Previous experiments in our lab have indicated that alcohol-mounted coverslipping of bone sections allows a better preservation at short and long term of the immunofluorescence signal than water-mounted coverslipping.

We have tested several antibodies raised against NGF to define what tumor associated stromal cells might express NGF protein as the ACE1-GFP tumor cells have been shown not to express mRNA for NGF using RT-PCR [19]. While many of the antibodies raised against NGF showed positive staining, none of this staining was specifically absorbed out using the blocking peptide. Thus in the present study, we were not able to determine which stromal cells express NGF by using immunohistochemistry.

2.6 Laser Confocal Microscopy

Images used were acquired with an Olympus Fluoview FV1000 and Carl Zeiss LSM 700. The endogenous GFP signal emitted from the prostate cancer cells did not require amplification for analysis. Sequential acquisition mode was used to reduce bleed-through from fluorophores. Differential interphase contrast images were simultaneously acquired with confocal images for GFP cancer cells by using the Carl Zeiss LSM700 system at 200 magnification. Images were automatically acquired with a motorized XY-scanning stage, with Mark & Find function (xyz) and assembled using Tile Scan (mosaic scan).

2.7 Quantification of the density of nerve fibers in tumor areas

For quantification purposes, cross sectional images of the whole bone (2 bone sections per animal) were obtained using a Carl Zeiss LSM 700 confocal system that is equipped with a computer-controlled motorized stage. For quantifying a particular marker, each cross section used for quantification was distant from the adjacent cross section by at least 0.1 mm. Density of nerve fibers per volume was obtained by determining the total length of nerve fibers using the curve spline tool (Axio Vision, v.4.8, Carl Zeiss) within the total area where only viable GFP cancer cells were present (leading edge of the tumor). Necrotic areas were defined as areas with cancer cells that did not fluoresce under an epi-fluorescent microscope with a filter to visualize GFP (band-pass emission filter from 500 to 530 nm). This result was then multiplied by the thickness of the longitudinal section to obtain the density of nerve fibers per volume.

2.8 Quantification of the vascularization and infiltration of macrophages in tumor area

Two confocal images (400x magnification) from three different bone sections per animal were captured. Bone sections were separated by at least 0.1 mm. Images of $CD68^+$ macrophages and $CD31^+$ blood vessels were acquired in areas where GFP^+ cancer cells were present. The average volume of bone with tumor cells that was analyzed was 315 μm (length), 315 μm (width) and 20 μm (depth). The Z-stacked gray-scale images were analyzed with Image-Pro Plus v. 6.0 (Media Cybernetics) and blood vessels were manually traced to determine the length of blood vessels within the tissue section. Neovascularization was reported as density of blood vessels per volume of tissue (mm/mm^3) [21]. $CD68^+$ macrophages were quantified in each layer of the tumor-bearing bone section from z-series images (400x magnification) of each field of view using Imaris Pro Software v. 6.0 (Bitplane AG, Zurich, Switzerland). Only $CD68^+$ cells that displayed visible nuclei as determined by counterstaining with DAPI were counted. Data from 3 bone sections per

mouse were acquired and averaged and results were expressed as total number of $CD68^+$ macrophages per tissue volume (mm^3).

2.9 Statistical analysis

Data are presented as mean ± SEM. The SPSS statistics package (v. 12, SPSS Inc) was used to perform statistical tests. Immunohistochemical and behavioral test groups were compared at each time point by one-way analysis of variance (ANOVA) followed by Fisher PLSD post-hoc comparisons. Significance level was set at $p<0.05$. In all cases, the investigator responsible for behavioral testing, plotting, measuring, and counting was blind to the experimental situation of each animal.

3. Results

3.1 Pathological bone remodeling and growth of cancer cells with disease progression

In the present study, we use a prostate cancer pain model that involves injecting and confining GFP^+ canine prostate cancer cells into the marrow space of the mouse femur and allowing the tumor cells to grow and remodel bone over an experimental time period of 70 days. Radiographic analysis of the tumor-injected femora showed that at day 35 post-cell injection, these prostate cancer cells induced bone-forming cancerous foci, which appear as nodular, rounded, and fairly well-circumscribed sclerotic areas due to the production of woven bone (Fig. 1B). As tumor growth progressed, the tumor associated pathological bone remodeling increased. This was similar to that reported in radiographs of human bones with metastatic prostate cancer at advances stages [5]. At day 70 post-cell injection (Fig. 1C), severe periosteal reaction (cortical bone reaction in response to a noxious insult) occurred as evidenced by a thick and disorganized appearance of the cortical bone and presence of the Codman's triangle (a triangular area of new sub-periosteal bone that is created when a tumor raises the periosteum away from the bone [5,45]). Six out of seven tumor-injected femurs presented Codman's triangle-like structures. Radiographic analysis indicated that bones from sham mice (needle placement + injection of culture medium) did not display significant bone remodeling (Fig. 1A) as compared to naïve mice (data not shown).

Immunohistochemical analysis was performed to define the association of GFP^+ cancer cells with other types of cells and determine the viability of prostate cancer cell colonies in the mouse bone. In femurs from sham mice (Fig 2A), the bone marrow is comprised of stacked hematopoetic cells (pink, Fig. 2A). At day 35 post-cell injection there is still bone marrow that is not occupied by cancer cells (pink). Simultaneous acquisition of differential interphase contrast (DIC) and confocal fluorescence images displayed the formation of new daughter cancer cell colonies (green) rounded by pathological woven bone (white/blue) at day 35 post-cell injection (Fig. 2B). At advanced stages of the disease (day 70), the entire bone marrow of the mouse femur was occupied by cancer cells. At day 70 post-tumor cell injection, the distribution and viability of GFP^+ cancer cells was not similar in the entire bone marrow. In sites where parent cancer cell colonies were initially formed, there were few viable GFP^+ cancer cells, but instead large necrotic areas (Fig. 2C), which is similar to what has been reported in human bones with metastatic prostate cancer at advanced stages [9]. At sites more distant from these necrotic areas (leading edge/viable areas of the tumor), there was formation of new daughter GFP^+ cancer cell colonies. Some of these daughter cancer cell colonies were observed in the interphase cortical bone/periosteum and were rounded by pathological woven bone (Fig. 2C).

3.2 Vascularization of the tumor-bearing femur with disease progression

In order to examine the distribution and structure of vascular elements, frozen bone sections of sham and tumor-injected femurs sacrificed at day 35 and day 70 post-cancer cell injection

were double-immunostained for the endothelial cell specific molecule PECAM and GFP^+ cancer cells. In sham mice, the blood vessels were observed to run longitudinally in the bone marrow and had a homogenous morphology (Fig. 3A). In contrast, at day 35 within the colonies of GFP^+ prostate cancer cells, there was an increase in the density of $PECAM^+$ blood vessels as compared to normal marrow space (Fig. 3B). Additionally, the tumor-associated blood vessels were different from those that vascularize normal bone marrow as they were thicker and exhibited disorganized, nonlinear morphology. At day 70 post cell injection, a high capillary density was maintained at the margin of the tumor of the prostate-injected femur (data not shown). However, a decline in blood vessel density was observed within the central necrotic areas of prostate cancer cell colonies (Fig. 3C). In contrast, in adjacent newly formed cancer cell colonies, there was a high density and chaotic vascularization (Fig. 3D).

3.3 Sprouting and organization of sensory and sympathetic nerve fibers in the bone marrow of the normal and prostate tumor-bearing bone

To examine the effects of prostate tumor growth on sensory innervation of the bone marrow, bone sections from naïve, sham and mice injected with GFP^+ prostate cancer cells sacrificed at different time points were labeled with an antibody raised against CGRP (Fig. 4), NF200 (Fig. 5), TH and TrkA. In comparing the organization and density of nerve fibers in the bone marrow of naïve (data not shown) versus sham mice, there appeared to be no difference in the organization or density of $CGRP^+$, $NF200^+$, TH^+ and $TrkA^+$ nerve fibers. Confocal images demonstrated that $CGRP^+$ (Fig. 4A) and $NF200^+$ (Fig. 5A) nerve fibers mainly run along the long axis of the bone as single nerve fibers with a largely linear morphology. The majority of $CGRP^+$ nerve fibers exhibited a beaded appearance (Fig. 4A). At day 35 post-cell injection in tumor-bearing mice, $CGRP^+$ (Fig. 4B), $NF200^+$ (Fig. 5B), TH^+ (data not shown) and $TrkA^+$ (data not shown) nerve fibers innervating the tumor cell colonies exhibited significant sprouting as evidenced by an increase in nerve fiber density and a highly disorganized appearance. These sprouting nerve fibers appeared to be intermingled among GFP^+ prostate cancer cells and the stromal cells that comprise the prostate cancer cell colonies (Fig. 4B, 5B). Similar to changes observed in the vascularization, at day 70 within the necrotic areas there was a significant reduction of $CGRP^+$ (Fig. 4C), $NF200^+$ (Fig. 5C), TH^+, and $TrkA^+$ nerve fibers. In contrast, in adjacent daughter cancer cell colonies, there was significant ectopic sprouting and formation of neuroma-like structures by $CGRP^+$ (Fig. 4D), $NF200^+$ (Fig. 5D), TH^+ and $TrkA^+$ nerve fibers (data not shown).

3.4 Systemic administration of anti-NGF therapy reduces tumor-induced nerve fiber sprouting and tumor-induced nociceptive behaviors

Previously, it was reported that prostate cancer cells induced a significant sprouting of CGRP and NF200 nerve fibers at day 28 post-cell injection, of which, the majority express TrkA [24]. Due to this finding, we evaluated the effect of anti-NGF on cancer cell-induced sprouting. Prostate cancer cell-injected mice treated with vehicle (day 14–day 70), early/sustained anti-NGF (day 14–day 70) and late/sustained anti-NGF (day 35–day 70) were sacrificed at day 70. Quantitative analysis was restricted only to those areas with viable cancer cell colonies. In tumor-injected mice treated with vehicle, there was significant ectopic sprouting of $CGRP^+$ (Fig. 6A) and $NF200^+$ nerve fibers (Fig. 6D) within and around the new cancer cell colonies. Both sustained anti-NGF treatment regimens resulted in attenuation of the $CGRP^+$ (Fig. 6B–C) and $NF200^+$ (Fig. 6E–F) nerve fiber sprouting. Quantitative analysis revealed that both anti-NGF treatment regimens prevented the sprouting of $CGRP^+$ (Fig. 7A), $NF200^+$ (Fig. 7B) and $TrkA^+$ (Fig. 7C) nerve fibers. Additionally, both anti-NGF treatment schedules significantly attenuated the sprouting of TH^+ nerve fibers. In sham animals the density of TH^+ nerve fibers was 87 ± 11 mm/mm^3 and increased in tumor-bearing mice treated with vehicle to 260 ± 36 mm/mm^3. Sustained

treatment with anti-NGF given from day 14 to day 70 and given from day 35 to day 70 reduced the tumor-induced nerve sprouting of TH^+ nerve fibers to 115 ± 27 mm/mm^3 and 52 ± 16 mm/mm^3, respectively.

Tumor-bearing mice displayed nociceptive behaviors (spontaneous guarding and flinching), which were first observed 14 days post-cell injection and then increased in severity with disease progression (Fig. 8). Minimal levels of nociceptive behaviors were observed in sham mice. To determine whether anti-NGF therapy attenuates bone cancer-induced nociception, nociceptive behaviors were analyzed in prostate tumor-bearing mice treated with vehicle, early/sustained anti-NGF or late/sustained anti-NGF, and compared to sham animals treated with vehicle. When anti-NGF was administered early/sustained, nociceptive behaviors were significantly reduced at nearly all time points evaluated (Fig. 8). When administration of anti-NGF was begun and sustained from day 35 to 70 (late/sustained), nociceptive behaviors were reduced significantly as compared to tumor-bearing mice treated with vehicle from day 42 to day 70 post-tumor injection. However, at some time points (day 42, 49, and 63), the anti-nociceptive effect produced by early/sustained administration of anti-NGF was significantly greater as compared to that produced by late/sustained administration of anti-NGF.

3.5 Systemic administration of anti-NGF does not affect tumor-induced bone remodeling, macrophage infiltration or neovascularization in the prostate cancer-bearing bones

The effects of anti-NGF therapy on bone formation and destruction were examined at day 70 post-tumor injection. Treatment of tumor-bearing mice with anti-NGF from day 14 to day 70 post-cancer cell injection resulted in no significant change in the pathological bone remodeling (Supplemental Fig. 1A–C) as evaluated by radiographic analysis. Immunohistochemical analysis was used to determine whether administration of anti-NGF significantly affects $PECAM^+$ aberrant neovascularization and $CD68^+$ macrophage infiltration in the bones inoculated with prostate cancer cells. Quantification of the total length of $PECAM^+$ blood vessels per tissue volume within the bone at day 70 post-tumor cell injection demonstrated that sustained anti-NGF treatment (day 14–day 70) does not significantly reduce the number of vessels as compared to vehicle treated animals (Supplemental figure 1D). Similarly, quantification of the total number of $CD68^+$ macrophages per tissue volume within the bone of tumor-bearing mice at day 70 post-tumor cell injection suggests that sustained anti-NGF treatment does not significantly reduce the number of macrophages as compared to vehicle treated animals (Supplemental Fig. 1E).

4. Discussion

4.1 Evolving mechanisms driving cancer pain

In the past decade there has been a significant increase in our knowledge of the mechanisms that drive cancer pain [33,39,48]. Currently, our understanding as to what drives cancer pain is that as tumor initially invades a tissue, nerve fibers that normally innervate that tissue are first activated/sensitized/injured by factors released by cancer and cancer-associated stromal/inflammatory/immune cells [33,48]. As the tumor continues to grow these “sensitized” nerve fibers detect and respond not only to noxious stimuli but also to normally non-noxious chemical, thermal or mechanical stimuli [33]. Thus, tumor-induced and/or released factors such as endothelins, prostaglandins, protons, bradykinin, NGF, cytokines (e.g. tumor necrosis factor, IL-6), and colony-stimulating factors have been shown to contribute to cancer pain [33,48,51].

While the above studies have been fruitful in providing “leads” for the development of novel therapies to treat cancer pain, several issues remain unexplained including whether

fundamentally different mechanisms drive ongoing versus breakthrough pain (breakthrough pain being defined as a transitory flare of extreme pain superimposed on an otherwise stable pain pattern [44]) and why there is frequently a poor correlation between tumor burden and the extent/severity of cancer pain [14,31,40]. For example, if sensory and sympathetic nerve fibers are "static" structures that simply respond to the changing tumor environment why are not all similar skeletal metastases painful and why is not there a clear correlation between tumor burden and pain? Recently, in breast [4], prostate [24], and sarcoma [34] models of bone cancer pain it has been shown that sensory and sympathetic nerve fibers that innervate the tumor-bearing organ undergo a highly active and pathological remodeling as the tumor and it's associated stromal cells invade the normal tissue. Additionally, *preventive* administration of anti-NGF or inhibition of TrkA blocked this tumor-induced nerve sprouting and neuroma formation [4,16,24,34]. Interestingly, the majority of NGF that is driving this sprouting appeared to be coming from tumor-associated stromal cells as the prostate cancer cell line, which induced the greatest extent of sprouting *in vivo* [24] is devoid of detectable mRNA coding for NGF [19].

What is remarkable about this tumor-induced remodeling of nerve fibers is not only how rapidly it occurs (within days to weeks), but the extent of the remodeling. Interestingly, many of the nerve fiber changes observed here are similar to changes that have been observed following nerve injury and nerve sprouting [11,28,60] where, similar to breakthrough cancer pain [36], the pain can be both severe, refractory to current medical treatment, and can have both a movement-evoked and spontaneous component [3,38].

4.2 Targeting the neuroplasticity of sensory and sympathetic nerve fibers for the relief of cancer pain

While above data has been useful in providing the beginning of an understanding to what drives cancer pain, the issue of tumor-induced sprouting and neuroma formation raised two fundamental questions that have significant mechanistic and therapeutic implications for cancer pain. First, if the parent cancer cell colonies are constantly evolving by proliferating, metastasizing and undergoing necrosis does this imply that the newly sprouted sensory and sympathetic nerve fibers that innervate the tumor-bearing organ are also constantly evolving? Secondly, it had been previously shown that when anti-NGF was given systemically to rats where the adult peripheral sensory nerve fibers were undergoing regeneration, further nerve regeneration is halted as long as anti-NGF was present but administration of anti-NGF did not show any sign of causing the withdrawal of nerve sprouting which had already occurred [12]. From a therapeutic perspective this is an important observation, since if tumor cells induced an ectopic sprouting and neuroma formation before blockade of NGF/TrkA is commenced in the cancer patient, can one expect this therapy to cause the withdrawal or disappearance of this ectopic sprouting and neuroma formation? Put another way, do you need to preemptively target the formation of this sprouting and neuroma formation for a blockade of NGF/TrkA therapy to be effective or can these therapies also be effective in middle to late stage cancer when the sprouting and neuroma formation has already occurred?

In this study we address this question using a prostate bone cancer pain model. The utility of this model is that it can be assessed to 70 days post-tumor injection at which time the parent cell colonies have proliferated and undergone necrosis, and nearby daughter cell colonies are viable and show no signs of necrosis. Robust sprouting is present by day 35 post-tumor injection. Using this model it is observed that exuberant nerve sprouting and neuroma formation occurs in colonies of viable cancer cells whether it be at the day 35 or 70 post-tumor cell injection. The populations of nerve fibers that are undergoing sprouting include $CGRP^+$ and $NF200^+$ sensory nerve fibers that correspond to unmyelinated/thinly myelinated and thinly myelinated nerve fibers, as well as TH^+ post-ganglionic sympathetic nerve fibers.

Importantly, a similar reduction in nociceptive behaviors, nerve sprouting and neuroma formation is observed whether sustained administration of anti-NGF was commenced early (days 14–70) or late (days 35–70). These results demonstrate that just as cancer cell colonies have a limited half-life, so do the sensory and sympathetic nerve fibers that innervate the tumor, as they sprout and form neuromas at the viable/leading edge of the tumor and then degenerate as the individual cancer cell colonies overgrow their blood flow and become necrotic (Fig 9). As most cancer cell colonies constantly proliferate, metastasize, and undergo necrosis, the present results suggest that early or late stage blockade of NGF/TrkA can attenuate both the ectopic nerve fiber reorganization and cancer pain.

4.3 Blockade of NGF/TrkA and the relief of human cancer pain

Several preclinical studies have shown that blocking NGF/TrkA can be efficacious in attenuating several types of malignant and non-malignant skeletal pain. Anti-NGF sequestering antibodies have been shown to reduce bone cancer pain due to sarcoma [34,52], breast [4] and prostate cancer [19,24] as well as in the painful arthritic knee joint [53], osteoarthritis [35], femoral fracture [25], and low back pain [26]. One rather unique aspect of the sensory innervation of bone and joint, which may partially explain why anti-NGF therapy is effective in relieving both malignant and non-malignant skeletal pain, is that greater than 80% of nerve fibers innervating bone are $TrkA^+$ fibers [7]. Whether targeting NGF/TrkA will be effective at reducing human cancer pain as well as other non-bony cancers and whether sprouting, neuroma formation of sensory and sympathetic nerve fibers also occurs in other frequently painful cancers such as head and neck cancer, or ovarian cancer remains to be determined.

Recent human trials with an anti-NGF therapy using humanized anti-NGF monoclonal antibodies also suggest that targeting NGF/TrkA can reduce skeletal pain [29,49]. In these studies, and in line with preclinical studies, anti-NGF therapy is anti-hyperalgesic (i.e. normalizing a decreased nociceptive threshold) as opposed to analgesic (i.e. increasing normal and sensitized nociceptive threshold). However, recent human clinical trials in elderly humans with OA have been halted due to the need for earlier than expected joint replacement in a small subset of patients [29,49]. What remains unclear is whether this earlier than expected joint replacement in patients being treated with anti-NGF is simply due to greater use of the diseased joint or to unforeseen adverse events on the bone itself such as a decrease in either the formation or maintenance of the vascular supply of the bone. While excessive relief of cancer pain is unlikely to be of significant concern for patients with advanced cancer, where blockade of NGF/TrkA has been reported to have a disease modifying effect on cancer, inhibition rather than promotion of cancer cell growth and metastasis has been observed [1,13,37,58].

4.3 Conclusions and limitations

The present results demonstrate that cancer pain is a “mixed pain” in that it has a nociceptive, neuropathic and tumorigenic component. Like the tumor itself, sensory and sympathetic nerve fibers appear to be continually evolving by undergoing sprouting, degeneration and re-sprouting with disease progression and this sprouting and neuroma formation and cancer pain is in part driven by NGF activation of $TrkA^+$ nerve fibers. These data suggest that this highly active and pathological sprouting and neuroma formation by the peripheral sensory and sympathetic nerve fibers may play a role in the extent, frequency and severity of cancer pain. The present results suggest that patients treated with early **or** late stage cancer may benefit from NGF/TrkA blocking therapies. Whether other painful cancers show similar sprouting of sensory and sympathetic nerve fibers, defining what specific stromal cells are the major source of NGF, determining whether removal of tumor-induced nerve sprouting and neuroma formation also reduce the central sensitization which occurs in

animals with cancer [27,50,55,59], defining the levels of receptors and ion channels expressed by newly sprouted nerve fibers and neuromas, and defining whether blockade of NGF/TrkA can reduce the proliferation and metastasis of specific types of cancer remain important, but unanswered questions.

Supplementary Material

Refer to Web version on PubMed Central for supplementary material.

Acknowledgments

This work was supported by the National Institutes of Health grant (NS23970, CA154550, CA157449), by the Department of Veteran Affairs, Veteran Health Administration, Rehabilitation Research and Development Service Grants (04380-I and A6707-R) and by the Calhoun Fund for Bone Pain. The authors thank Magdalena J. Kaczmarska, Aaron Bloom, Katie T. Freeman and Kathleen Coughlin for their excellent technical assistance.

References

1. Adriaenssens E, Vanhecke E, Saule P, Mougel A, Page A, Romon R, Nurcombe V, Le Bourhis X, Hondermarck H. Nerve growth factor is a potential therapeutic target in breast cancer. Cancer Res. 2008; 68(2):346–351. [PubMed: 18199526]
2. Ayala GE, Wheeler TM, Shine HD, Schmelz M, Frolov A, Chakraborty S, Rowley D. In vitro dorsal root ganglia and human prostate cell line interaction: redefining perineural invasion in prostate cancer. Prostate. 2001; 49(3):213–223. [PubMed: 11746267]
3. Black JA, Nikolajsen L, Kroner K, Jensen TS, Waxman SG. Multiple sodium channel isoforms and mitogen-activated protein kinases are present in painful human neuromas. Ann Neurol. 2008; 64(6): 644–653. [PubMed: 19107992]
4. Bloom AP, Jimenez-Andrade JM, Taylor RN, Castaneda-Corral G, Kaczmarska MJ, Freeman KT, Coughlin KA, Ghilardi JR, Kuskowski MA, Mantyh PW. Breast Cancer-Induced Bone Remodeling, Skeletal Pain and Sprouting of Sensory Nerve Fibers. J Pain. 2011
5. Bloom RA, Libson E, Husband JE, Stoker DJ. The periosteal sunburst reaction to bone metastases. A literature review and report of 20 additional cases. Skeletal Radiol. 1987; 16(8):629–634. [PubMed: 3321463]
6. Caltagirone C, Spoletini I, Gianni W, Spalletta G. Inadequate pain relief and consequences in oncological elderly patients. Surg Oncol. 2010; 19(3):178–183. [PubMed: 20015635]
7. Castaneda-Corral G, Jimenez Andrade JM, Bloom AP, Taylor RN, Mantyh WG, Kaczmarksa MJ, Ghilardi JR, Mantyh PW. The majority of myelinated and unmyelinated sensory nerve fibers that innervate bone express TrkA. Neuroscience. 2011; 178:196–207. [PubMed: 21277945]
8. Ceyhan GO, Bergmann F, Kadihasanoglu M, Altintas B, Demir IE, Hinz U, Muller MW, Giese T, Buchler MW, Giese NA, Friess H. Pancreatic neuropathy and neuropathic pain-a comprehensive pathomorphological study of 546 cases. Gastroenterology. 2009; 136(1):177–186. e171. [PubMed: 18992743]
9. Cheville JC, Tindall D, Boelter C, Jenkins R, Lohse CM, Pankratz VS, Sebo TJ, Davis B, Blute ML. Metastatic prostate carcinoma to bone: clinical and pathologic features associated with cancer-specific survival. Cancer. 2002; 95(5):1028–1036. [PubMed: 12209687]
10. Costantini M, Ripamonti C, Beccaro M, Montella M, Borgia P, Casella C, Miccinesi G. Prevalence, distress, management, and relief of pain during the last 3 months of cancer patients' life. Results of an Italian mortality follow-back survey. Ann Oncol. 2009; 20(4):729–735. [PubMed: 19164455]
11. Devor M, Govrin-Lippmann R, Angelides K. Na+ channel immunolocalization in peripheral mammalian axons and changes following nerve injury and neuroma formation. J Neurosci. 1993; 13(5):1976–1992. [PubMed: 7683047]
12. Diamond J, Holmes M, Coughlin M. Endogenous NGF and nerve impulses regulate the collateral sprouting of sensory axons in the skin of the adult rat. J Neurosci. 1992; 12(4):1454–1466. [PubMed: 1556603]

13. Dionne CA, Camoratto AM, Jani JP, Emerson E, Neff N, Vaught JL, Murakata C, Djakiew D, Lamb J, Bova S, George D, Isaacs JT. Cell cycle-independent death of prostate adenocarcinoma is induced by the trk tyrosine kinase inhibitor CEP-751 (KT6587). Clin Cancer Res. 1998; 4(8): 1887–1898. [PubMed: 9717816]
14. Front D, Schneck SO, Frankel A, Robinson E. Bone metastases and bone pain in breast cancer. Are they closely associated? Jama. 1979; 242(16):1747–1748. [PubMed: 480600]
15. Gerbershagen HJ, Ozgur E, Straub K, Dagtekin O, Gerbershagen K, Petzke F, Heidenreich A, Lehmann KA, Sabatowski R. Prevalence, severity, and chronicity of pain and general health-related quality of life in patients with localized prostate cancer. Eur J Pain. 2008; 12(3):339–350. [PubMed: 17855135]
16. Ghilardi JR, Freeman KT, Jimenez-Andrade JM, Mantyh GW, Bloom AP, Kuskowski MA, Mantyh PW. Administration of a tropomyosin receptor kinase inhibitor attenuates sarcoma-induced nerve sprouting, neuroma formation and bone cancer pain. Molecular Pain. 2010; 6(87)
17. Ghilardi JR, Rohrich H, Lindsay TH, Sevcik MA, Schwei MJ, Kubota K, Halvorson KG, Poblete J, Chaplan SR, Dubin AE, Carruthers NI, Swanson D, Kuskowski M, Flores CM, Julius D, Mantyh PW. Selective blockade of the capsaicin receptor TRPV1 attenuates bone cancer pain. J Neurosci. 2005; 25(12):3126–3131. [PubMed: 15788769]
18. Halvorson KG, Kubota K, Sevcik MA, Lindsay TH, Sotillo JE, Ghilardi JR, Rosol TJ, Boustany L, Shelton DL, Mantyh PW. A blocking antibody to nerve growth factor attenuates skeletal pain induced by prostate tumor cells growing in bone. Cancer Res. 2005; 65(20):9426–9435. [PubMed: 16230406]
19. Halvorson KG, Kubota K, Sevcik MA, Lindsay TH, Sotillo JE, Ghilardi JR, Rosol TJ, Boustany L, Shelton DL, Mantyh PW. A blocking antibody to nerve growth factor attenuates skeletal pain induced by prostate tumor cells growing in bone. Cancer Res. 2005; 65(20):9426–9435. [PubMed: 16230406]
20. Hongo JS, Laramee GR, Urfer R, Shelton DL, Restivo T, Sadick M, Galloway A, Chu H, Winslow JW. Antibody binding regions on human nerve growth factor identified by homolog- and alanine-scanning mutagenesis. Hybridoma. 2000; 19(3):215–227. [PubMed: 10952410]
21. Honore P, Mantyh PW. Bone cancer pain: from mechanism to model to therapy. Pain Med. 2000; 1(4):303–309. [PubMed: 15101876]
22. Jemal A, Bray F, Center MM, Ferlay J, Ward E, Forman D. Global cancer statistics. CA Cancer J Clin. 2011; 61(2):69–90. [PubMed: 21296855]
23. Jemal A, Siegel R, Xu J, Ward E. Cancer statistics, 2010. CA Cancer J Clin. 2010; 60(5):277–300. [PubMed: 20610543]
24. Jimenez-Andrade JM, Bloom AP, Stake JI, Mantyh WG, Taylor RN, Freeman KT, Ghilardi JR, Kuskowski MA, Mantyh PW. Pathological sprouting of adult nociceptors in chronic prostate cancer-induced bone pain. J Neurosci. 2010; 30(44):14649–14656. [PubMed: 21048122]
25. Jimenez-Andrade JM, Martin CD, Koewler NJ, Freeman KT, Sullivan LJ, Halvorson KG, Barthold CM, Peters CM, Buus RJ, Ghilardi JR, Lewis JL, Kuskowski MA, Mantyh PW. Nerve growth factor sequestering therapy attenuates non-malignant skeletal pain following fracture. Pain. 2007; 133(1–3):183–196. [PubMed: 17693023]
26. Katz N, Borenstein DG, Birbara C, Bramson C, Nemeth MA, Smith MD, Brown MT. Efficacy and safety of tanezumab in the treatment of chronic low back pain. Pain. 2011
27. Khasabov SG, Hamamoto DT, Harding-Rose C, Simone DA. Tumor-evoked hyperalgesia and sensitization of nociceptive dorsal horn neurons in a murine model of cancer pain. Brain Res. 2007; 1180:7–19. [PubMed: 17935703]
28. Kryger GS, Kryger Z, Zhang F, Shelton DL, Lineaweaver WC, Buncke HJ. Nerve growth factor inhibition prevents traumatic neuroma formation in the rat. J Hand Surg Am. 2001; 26(4):635–644. [PubMed: 11466637]
29. Lane NE, Schnitzer TJ, Birbara CA, Mokhtarani M, Shelton DL, Smith MD, Brown MT. Tanezumab for the treatment of pain from osteoarthritis of the knee. N Engl J Med. 2010; 363(16): 1521–1531. [PubMed: 20942668]

30. LeRoy BE, Thudi NK, Nadella MV, Toribio RE, Tannehill-Gregg SH, van Bokhoven A, Davis D, Corn S, Rosol TJ. New bone formation and osteolysis by a metastatic, highly invasive canine prostate carcinoma xenograft. Prostate. 2006; 66(11):1213–1222. [PubMed: 16683269]
31. Levren G, Sadik M, Gjertsson P, Lomsky M, Michanek A, Edenbrandt L. Relation between pain and skeletal metastasis in patients with prostate or breast cancer. Clin Physiol Funct Imaging. 2010
32. Lindsay TH, Jonas BM, Sevcik MA, Kubota K, Halvorson KG, Ghilardi JR, Kuskowski MA, Stelow EB, Mukherjee P, Gendler SJ, Wong GY, Mantyh PW. Pancreatic cancer pain and its correlation with changes in tumor vasculature, macrophage infiltration, neuronal innervation, body weight and disease progression. Pain. 2005; 119(1–3):233–246. [PubMed: 16298491]
33. Mantyh PW. Cancer pain and its impact on diagnosis, survival and quality of life. Nat Rev Neurosci. 2006; 7(10):797–809. [PubMed: 16988655]
34. Mantyh WG, Jimenez-Andrade JM, Stake JI, Bloom AP, Kaczmarska MJ, Taylor RN, Freeman KT, Ghilardi JR, Kuskowski MA, Mantyh PW. Blockade of nerve sprouting and neuroma formation markedly attenuates the development of late stage cancer pain. Neuroscience. 2010; 171(2):588–598. [PubMed: 20851743]
35. McNamee KE, Burleigh A, Gompels LL, Feldmann M, Allen SJ, Williams RO, Dawbarn D, Vincent TL, Inglis JJ. Treatment of murine osteoarthritis with TrkAd5 reveals a pivotal role for nerve growth factor in non-inflammatory joint pain. Pain. 2010; 149(2):386–392. [PubMed: 20350782]
36. Mercadante S, Arcuri E. Breakthrough pain in cancer patients: pathophysiology and treatment. Cancer Treat Rev. 1998; 24(6):425–432. [PubMed: 10189409]
37. Miknyoczki SJ, Wan W, Chang H, Dobrzanski P, Ruggeri BA, Dionne CA, Buchkovich K. The neurotrophin-trk receptor axes are critical for the growth and progression of human prostatic carcinoma and pancreatic ductal adenocarcinoma xenografts in nude mice. Clin Cancer Res. 2002; 8(6):1924–1931. [PubMed: 12060637]
38. Montagnini ML, Zaleon CR. Pharmacological management of cancer pain. J Opioid Manag. 2009; 5(2):89–96. [PubMed: 19507805]
39. Pacharinsak C, Beitz A. Animal models of cancer pain. Comp Med. 2008; 58(3):220–233. [PubMed: 18589864]
40. Palmer E, Henrikson B, McKusick K, Strauss HW, Hochberg F. Pain as an indicator of bone metastasis. Acta Radiol. 1988; 29(4):445–449. [PubMed: 3408606]
41. Pelger RC, Soerdjbalie-Maikoe V, Hamdy NA. Strategies for management of prostate cancer-related bone pain. Drugs Aging. 2001; 18(12):899–911. [PubMed: 11888345]
42. Peters CM, Ghilardi JR, Keyser CP, Kubota K, Lindsay TH, Luger NM, Mach DB, Schwei MJ, Sevcik MA, Mantyh PW. Tumor-induced injury of primary afferent sensory nerve fibers in bone cancer pain. Exp Neurol. 2005; 193(1):85–100. [PubMed: 15817267]
43. Pollen JJ, Schmidt JD. Bone pain in metastatic cancer of prostate. Urology. 1979; 13(2):129–134. [PubMed: 433019]
44. Portenoy RK, Hagen NA. Breakthrough pain: definition, prevalence and characteristics. Pain. 1990; 41(3):273–281. [PubMed: 1697056]
45. Rana RS, Wu JS, Eisenberg RL. Periosteal reaction. AJR Am J Roentgenol. 2009; 193(4):W259–272. [PubMed: 19770293]
46. Sabino MA, Ghilardi JR, Jongen JL, Keyser CP, Luger NM, Mach DB, Peters CM, Rogers SD, Schwei MJ, de Felipe C, Mantyh PW. Simultaneous reduction in cancer pain, bone destruction, and tumor growth by selective inhibition of cyclooxygenase-2. Cancer Res. 2002; 62(24):7343–7349. [PubMed: 12499278]
47. Sandblom G, Carlsson P, Sigsjo P, Varenhorst E. Pain and health-related quality of life in a geographically defined population of men with prostate cancer. Br J Cancer. 2001; 85(4):497–503. [PubMed: 11506486]
48. Schmidt BL, Hamamoto DT, Simone DA, Wilcox GL. Mechanism of cancer pain. Mol Interv. 2010; 10(3):164–178. [PubMed: 20539035]
49. Schnitzer TJ, Lane NE, Birbara C, Smith MD, Simpson SL, Brown MT. Long-term open-label study of tanezumab for moderate to severe osteoarthritic knee pain. Osteoarthritis Cartilage. 2011

50. Schwei MJ, Honore P, Rogers SD, Salak-Johnson JL, Finke MP, Ramnaraine ML, Clohisy DR, Mantyh PW. Neurochemical and cellular reorganization of the spinal cord in a murine model of bone cancer pain. J Neurosci. 1999; 19(24):10886–10897. [PubMed: 10594070]
51. Schweizerhof M, Stosser S, Kurejova M, Njoo C, Gangadharan V, Agarwal N, Schmelz M, Bali KK, Michalski CW, Brugger S, Dickenson A, Simone DA, Kuner R. Hematopoietic colony-stimulating factors mediate tumor-nerve interactions and bone cancer pain. Nat Med. 2009; 15(7): 802–807. [PubMed: 19525966]
52. Sevcik MA, Ghilardi JR, Peters CM, Lindsay TH, Halvorson KG, Jonas BM, Kubota K, Kuskowski MA, Boustany L, Shelton DL, Mantyh PW. Anti-NGF therapy profoundly reduces bone cancer pain and the accompanying increase in markers of peripheral and central sensitization. Pain. 2005; 115(1–2):128–141. [PubMed: 15836976]
53. Shelton DL, Zeller J, Ho WH, Pons J, Rosenthal A. Nerve growth factor mediates hyperalgesia and cachexia in auto-immune arthritis. Pain. 2005; 116(1–2):8–16. [PubMed: 15927377]
54. Soebadi RD, Tejawinata S. Indonesia: status of cancer pain and palliative care. J Pain Symptom Manage. 1996; 12(2):112–115. [PubMed: 8754994]
55. Urch CE, Donovan-Rodriguez T, Dickenson AH. Alterations in dorsal horn neurones in a rat model of cancer-induced bone pain. Pain. 2003; 106(3):347–356. [PubMed: 14659517]
56. van den Beuken-van Everdingen MH, de Rijke JM, Kessels AG, Schouten HC, van Kleef M, Patijn J. Prevalence of pain in patients with cancer: a systematic review of the past 40 years. Ann Oncol. 2007; 18(9):1437–1449. [PubMed: 17355955]
57. Wacnik PW, Baker CM, Herron MJ, Kren BT, Blazar BR, Wilcox GL, Hordinsky MK, Beitz AJ, Ericson ME. Tumor-induced mechanical hyperalgesia involves CGRP receptors and altered innervation and vascularization of DsRed2 fluorescent hindpaw tumors. Pain. 2005; 115(1–2):95–106. [PubMed: 15836973]
58. Warrington RJ, Lewis KE. Natural antibodies against nerve growth factor inhibit in vitro prostate cancer cell metastasis. Cancer Immunol Immunother. 2011; 60(2):187–195. [PubMed: 20976447]
59. Yanagisawa Y, Furue H, Kawamata T, Uta D, Yamamoto J, Furuse S, Katafuchi T, Imoto K, Iwamoto Y, Yoshimura M. Bone cancer induces a unique central sensitization through synaptic changes in a wide area of the spinal cord. Mol Pain. 2010; 6:38. [PubMed: 20602757]
60. Yen LD, Bennett GJ, Ribeiro-da-Silva A. Sympathetic sprouting and changes in nociceptive sensory innervation in the glabrous skin of the rat hind paw following partial peripheral nerve injury. J Comp Neurol. 2006; 495(6):679–690. [PubMed: 16506190]
61. Zimmermann M. Ethical guidelines for investigations of experimental pain in conscious animals. Pain. 1983; 16:109–110. [PubMed: 6877845]

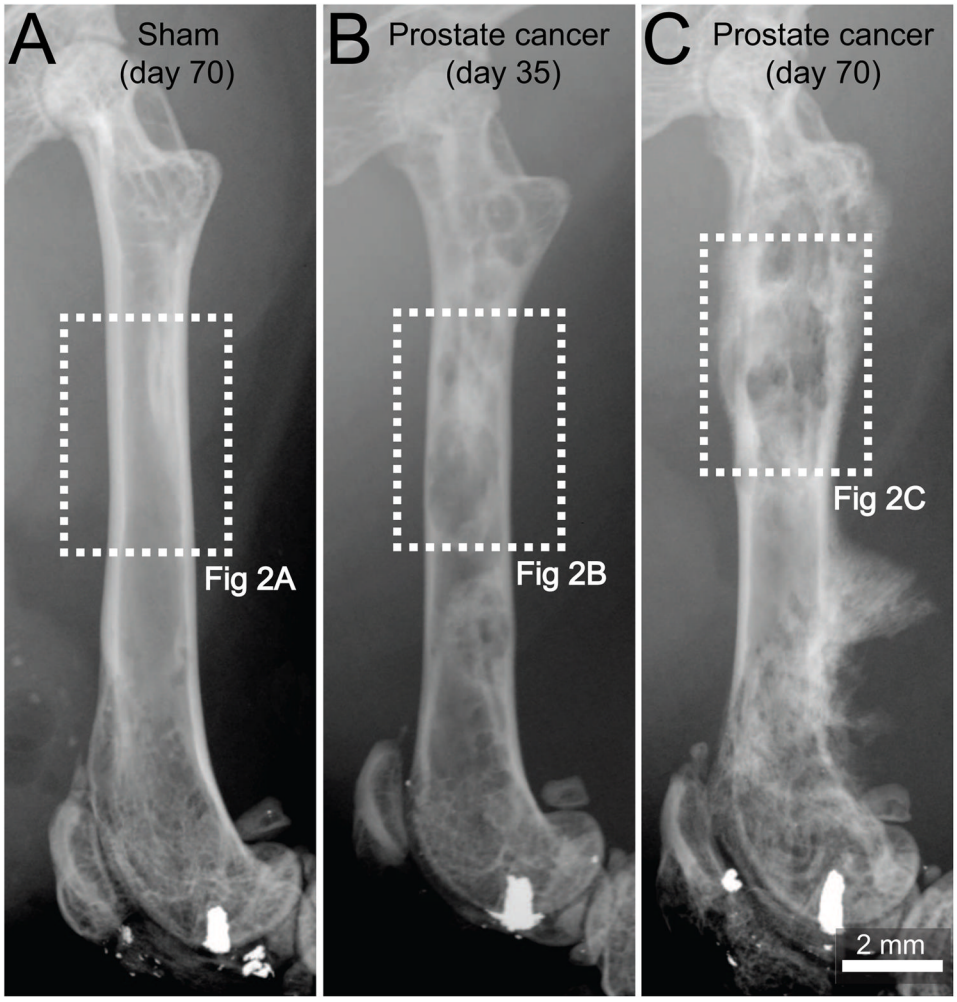

Figure 1. Pathological bone remodeling induced by prostate cancer cells growing within the femur

Representative radiographic images of a mouse femur at day 70 following injection of culture medium alone (sham, A), at day 35 following injection of ACE-1 prostate cancer cells (B) or day 70 following injection of prostate cancer cells (C). At day 35 post-cancer cell injection the tumor-injected mouse femur shows osteoblastic lesions, characterized by pathological bone formation in the intramedullary space, which generate diaphyseal bridging structures (B). Note that by day 70, the osteoblastic lesions increase in magnitude and an aggressive periosteal reaction is evidenced as a dense and disorganized appearance of the cortical bone in the distal methaphysis and formation of a Codman's triangle-like structure in the distal diaphysis (C). A Codman's triangle develops when a portion of periosteum is lifted off of the cortex by tumor and has been reported to occur in bones from patients with metastatic prostate cancer. Sham-injected femurs show no evidence of bone formation or bone destruction (A). Dashed line rectangles in white represent the areas of the bones illustrated in figure 2.

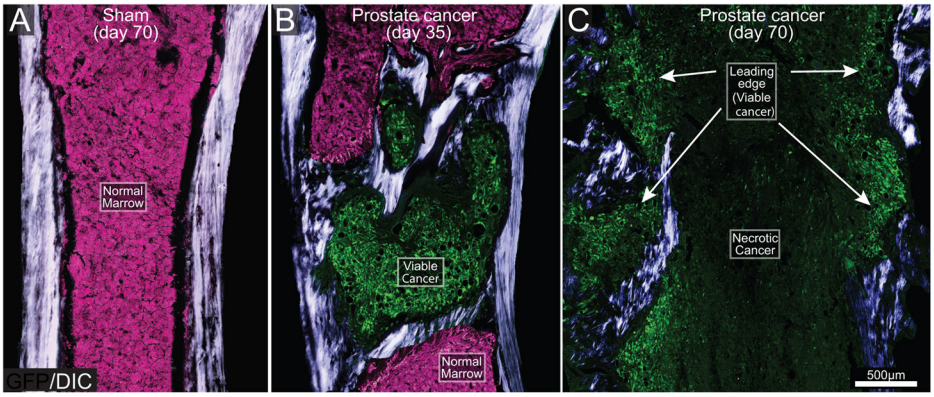

Figure 2. The evolving histopathology as prostate cancer cells grow within the mouse femur

Differential interphase contrast (DIC) images overlaid on confocal green fluorescent protein (GFP) images (20 μm-thick) of a sham (A) and prostate cancer cell-injected femur from mice sacrificed at days 35 (B) and 70 (C) post-cancer cell injection. DIC images were acquired to visualize cortical and pathological woven bone. As the GFP^+ tumor cells (green) grow in normal bone marrow (normal tightly packed hematopoietic cells, pink) they induce the formation of woven bone around the tumor cell colony and eventually form an osteoblastic lesion (B). As tumor disease progresses (day 70), the parent cancer cell colonies undergo necrosis, whereas viable, daughter cancer cell colonies, which are also surrounded by new bone, form at sites more distant from bone marrow (C). Note that at late stages of the disease, the diameter of the femur is greater than that of the femur at day 35 post-tumor injection, or sham bones due to the continuous bone growth induced by prostate cancer cells. Note that osteoblastic lesions are not present in the sham femur (A). For illustration purposes, the background signal which corresponds to healthy bone marrow is presented as the color pink and the GFP^+ tumor cells as green.

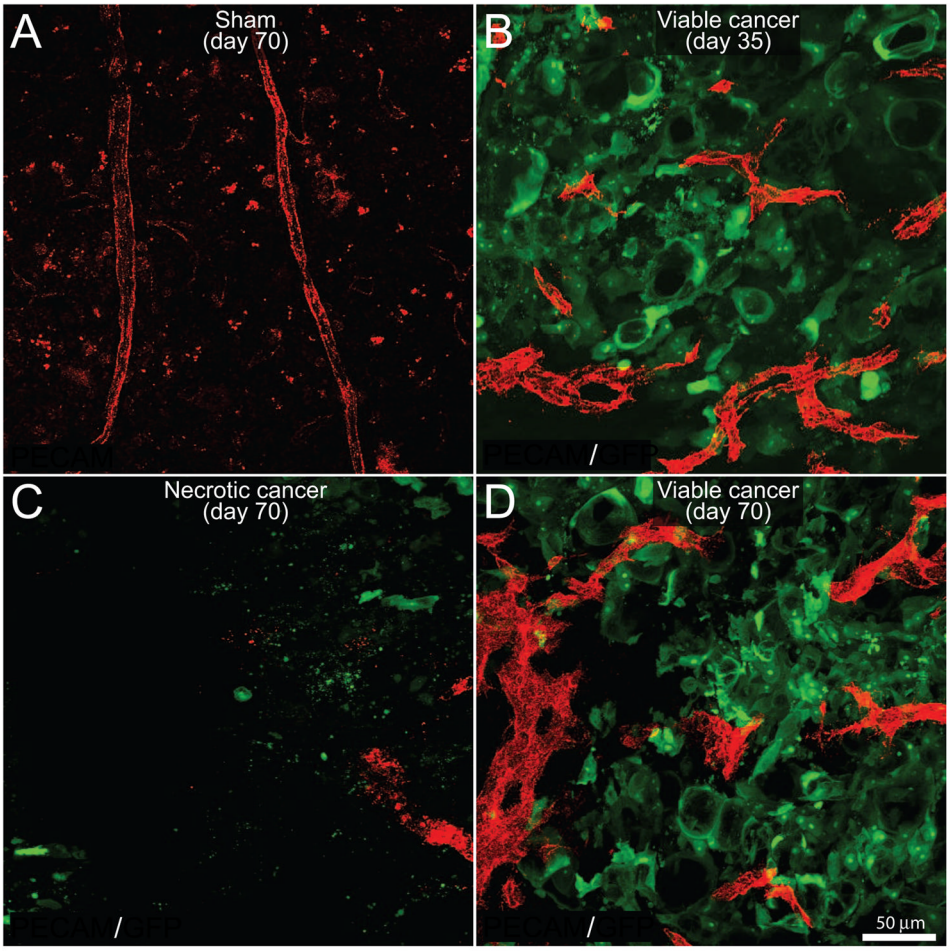

Figure 3. Newly formed prostate cancer cell colonies are highly viable and well vascularized whereas older cancer cell colonies lose their vascular supply and undergo necrosis and death

Confocal images of bone sections (20 µm-thick) from sham mice (A) or mice sacrificed at days 35 (B) or 70 (C,D) post-tumor cell injection. GFP^+ cancer cell (green)-bearing bone sections were immunostained with an antibody against the platelet endothelial cell adhesion molecule (PECAM, red) to immunolabel endothelial cells of blood vessels. Blood vessels in the bone marrow in naïve (data not shown) and sham injected animals (A) have a highly organized, homogenous and mostly linear morphology. As GFP^+ prostate tumor cells grow within the bone (B), there is an increase in the density of $PECAM^+$ blood vessels (red) inside and immediately surrounding the cancer cell colonies. Note that these $PECAM^+$ blood vessels have a highly heterogeneous and disorganized morphology as compared to blood vessels in the bone marrow of sham mice (B). At day 70, the older cancer cell colonies show a loss of $PECAM^+$ blood vessels and as well as GFP^+ cancer cells (C), whereas the immediately adjacent daughter cancer colonies are characterized by a high density of $PECAM^+$ blood vessels and GFP^+ cancer cells (D). Images were acquired at the metaphyseal region of the bone marrow and were projected from 40 optical sections at 0.5 µm intervals.

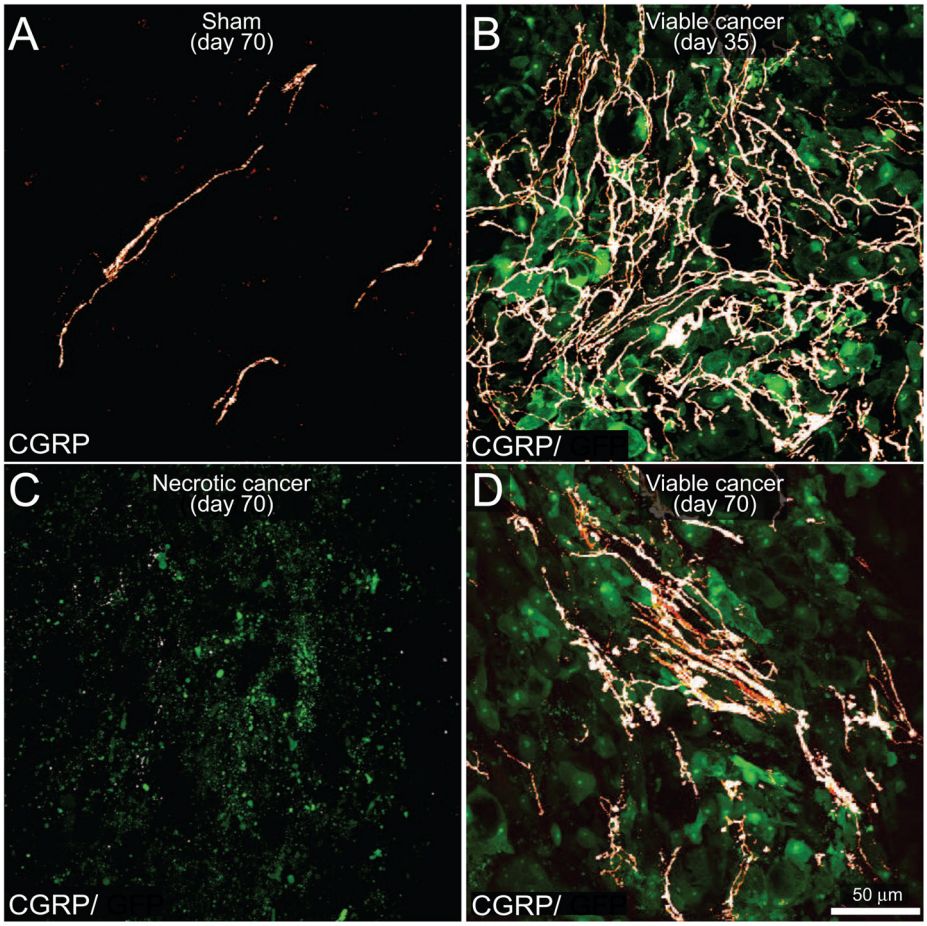

Figure 4. The evolving reorganization of CGRP$^+$ sensory nerve fibers with disease progression

Confocal images of bone sections (20 μm-thick) from sham mice (A) or mice sacrificed at days 35 (B) or 70 (C,D) post prostate tumor cells injection. GFP$^+$ cancer cell (green)-bearing bone sections were immunostained with an antibody against calcitonin gene-related peptide (CGRP, a marker of peptide-rich sensory nerve fibers, white). Note that in the sham mice (A), CGRP$^+$ nerve fibers that innervate the healthy marrow space appear as single nerve fibers with a highly linear morphology. In contrast, as GFP$^+$ prostate tumor cells proliferate and form tumor colonies (day 35 post-cell injection; B), the CGRP$^+$ sensory nerve fibers undergo marked sprouting as characterized by an increased density, highly branched architecture, and disorganized morphology as compared to nerve fibers innervating the marrow space in sham animals (A). At day 70 post-cell injection the older parent cancer cell colonies show signs of necrosis as evidenced by a loss of GFP expression in the cancer cells, as well as a decrease in the density of CGRP$^+$ nerve fibers (C), whereas adjacent newly formed daughter cancer colonies show robust sprouting and formation of neuroma-like structures by CGRP$^+$ nerve fibers (D). Images were acquired at the metaphyseal region of the bone marrow and were projected from 40 optical sections at 0.5 μm intervals.

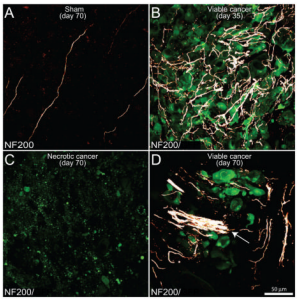

Figure 5. The evolving reorganization of NF200$^+$ sensory nerve fibers as prostate cancer cells proliferate, metastasize and undergo necrosis in the mouse femur

Confocal images of bone sections (20 μm-thick) from sham mice (A) or mice sacrificed at days 35 (B) or 70 (C,D) post-injection. GFP$^+$ cancer cell (green)-bearing bone sections were incubated with an antibody against 200 kD neurofilament (NF200, a marker of myelinated nerve fibers; white). Note that in the sham mice (A), NF200$^+$ nerve fibers that innervate the healthy marrow space appear as single nerve fibers with a highly linear morphology. In contrast, as GFP$^+$ prostate tumor cells proliferate and form tumor colonies at day 35 post-cell injection (B), the NF200$^+$ sensory nerve fibers undergo marked sprouting characterized by a highly branched morphology and increased density as compared to sham mice. With time, older parent colonies show a dramatic loss of GFP$^+$ cancer cells, as well as a decrease in the density of NF200$^+$ nerve fibers (C), whereas immediately adjacent new daughter cancer cell colonies show robust expression of GFP as well as sprouting and formation of neuroma-like structures (arrow) by NF200 nerve fibers (D). Images were acquired at the metaphyseal region of the bone marrow and were projected from 40 optical sections at 0.5 μm intervals.

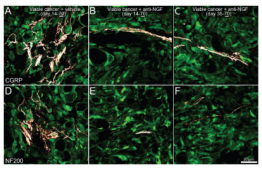

Figure 6. Sustained treatment with anti-NGF, given either preemptively or late in disease progression, decreases tumor-induced sprouting of CGRP$^+$ and NF200$^+$ sensory nerve fibers

Representative confocal images of viable cancer cell colonies of bones harvested from mice sacrificed at day 70 post-prostate tumor cell injection (underline of 70). With advanced disese progression prostate cancer cells (which are transfected with green fluorescent protein: GFP, green) form new viable colonies of cancer cells, in which there is dramatic sprouting and formation of neuroma-like structures by CGRP$^+$ (A) and NF200$^+$ (D) nerve fibers. Preemptive, sustained sequestration of NGF (10 mg/kg; i.p., administered from day 14 to day 70) or late administration (given from day 35 to day 70 post-cancer cell injection) significantly reduces the pathological tumor-induced sprouting and formation of neuroma-like structures of sensory CGRP$^+$ (B, C) and NF200$^+$ (E, F) nerve fibers at day 70 post-tumor injection. Images were acquired at the metaphyseal region of the bone marrow and were projected from 40 optical sections at 0.5 μm intervals.

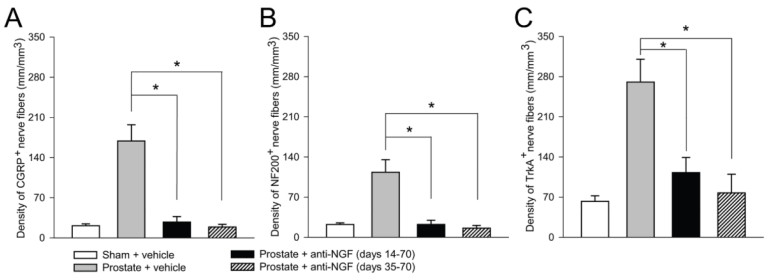

Figure 7. Histograms showing that sustained administration of NGF sequestering therapy, given either early or late in disease progression, reduces prostate-induced nerve sprouting of CGRP$^+$, NF200$^+$, and TrkA$^+$ nerve fibers

At day 70 post cell injection, the density of CGRP$^+$ (A), NF200$^+$ (B), and TrkA$^+$ (C) nerve fibers is significantly greater in prostate + vehicle-treated mice compared to sham + vehicle-treated mice. At day 70 post-tumor injection, tumor-induced nerve sprouting is significantly attenuated by preemptive/sustained administration or anti-NGF (10 mg/kg; i.p., given from day 14 to day 70 post-cell injection) or by late/sustained administration of anti-NGF (10 mg/kg; i.p., given from day 35 to day 70 post-cell injection). Nerve fiber density was determined by measuring the total length of nerve fibers in areas where viable cancer cells were present. Brackets indicate the groups being compared. *$p<0.05$. Bars represent the mean ± SEM for at minimum six mice.

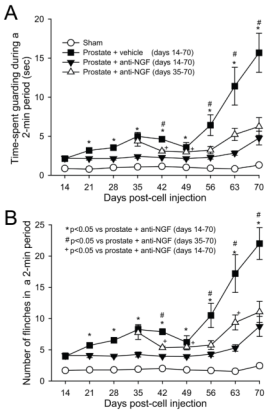

Figure 8. Anti-NGF treatment, when given early or late in disease progression, attenuates prostate cancer-induced nociceptive behaviors

Nociceptive behaviors including spontaneous guarding (A) and flinching (B) recorded in sham mice (needle placement + injection of culture medium), prostate cancer-bearing mice treated with vehicle, prostate cancer-bearing mice treated preemptively with anti-NGF (from days 14 to 70 post-cell injection) and prostate cancer mice treated late with anti-NGF (from days 35 to 70 post-cell injection). Note that nociceptive behaviors in tumor-bearing mice are evident by day 14 post-cell injection and are significantly greater than sham mice at all time points shown. Preemptive sustained treatment with anti-NGF which was commenced at day 14 post-tumor cell injection significantly decreased nociceptive behaviors. Importantly, late sustained treatment with anti-NGF which was commenced at day 35 post-tumor injection (when robust sprouting in the parent cell colonies has already occurred) also decreased the nociceptive behaviors. Anti-NGF was given every 5 days (10 mg/kg, i.p.) and each point represents the mean ± SEM.

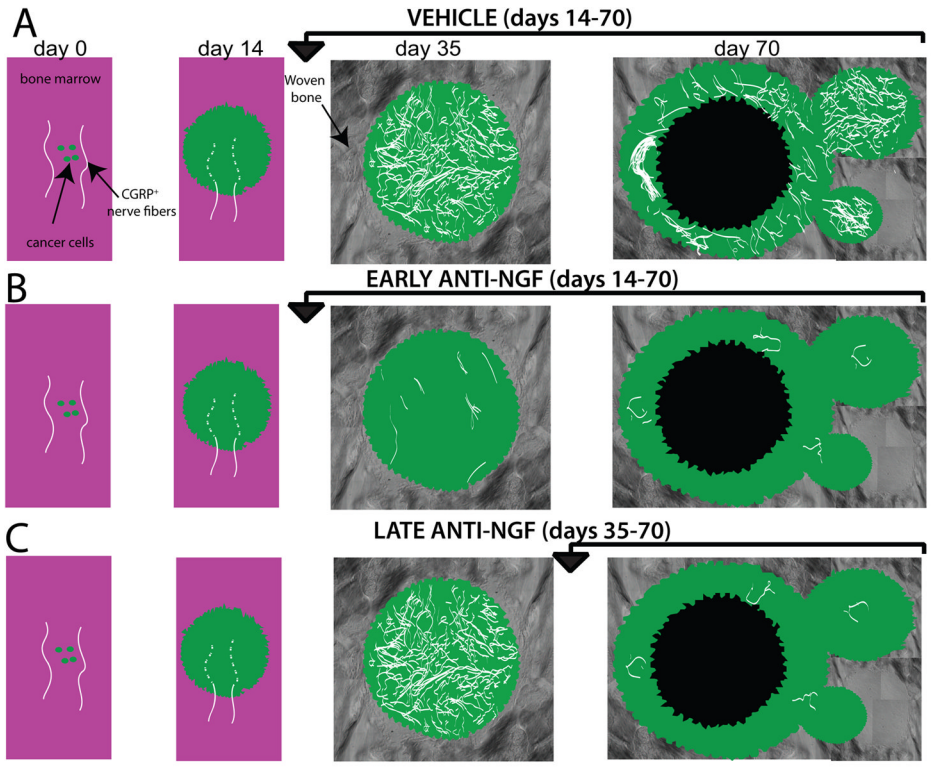

Figure 9. Schematic illustrating the effect that preemptive or late administration of anti-NGF has on nerve fiber pathology with prostate cancer disease progression in bone

A) Following initial injection and confinement of the prostate tumor cells into the marrow space of the femur, there are small cancer cell colonies composed mainly of proliferating cancer cells that are innervated only by the sensory nerve fibers that normally innervate the bone, which have a linear and regular morphology. As the prostate tumor cells proliferate within the bone marrow (day 14) the tumor cells activate, injure and then destroy the very distal processes of sensory fibers that innervate the bone marrow (dashed lines). By day 35 post-tumor cell injection the cancer cells colonies (which are now composed of both cancer cells and their associate stromal cells) increase in size and are surrounded by copious amounts of newly formed woven bone, which has been induced by the prostate cancer colony. At this time point there is a clear remodeling of $TrkA^+$ sensory and sympathetic nerve fibers and this reorganization is characterized by an increased density of nerve fibers which are highly branched and have a disorganized morphology that is never observed in the normal marrow space. At late stages of the disease (day 70) the sensory and sympathetic nerve fibers that innervate the viable, well vascularized daughter cell colonies show significant sprouting and neuroma formation whereas there is little evidence of any sensory or sympathetic nerve fibers innervating the older, now necrotic parent cancer cell colonies. Early and sustained anti-NGF therapy (day 14–70 day post-tumor cell injection) prevents sprouting and neuroma formation throughout the time the therapy is administered. In contrast, sustained anti-NGF treatment (day 35–70) prevents the nerve sprouting and neuroma formation which normally occur in the later formed daughter cell colonies, which are the only viable cell colonies that are present in the tumor-bearing bone at day 70 post-tumor injection.